Materials Research. 2021; 24(5): e20210202
DOI: https://doi.org/10.1590/1980-5373-MR-2021-0202

Investigation of Spark Erosion Behavior of Rene 41 Alloy Using Powder Mixed Dielectric Fluid

S. Sabareesan[a]*, D. Vasudevan[a]

[a]PSNA College of Engineering and Technology, Department of Mechanical Engineering, Dindigul - 624622, Tamilnadu, India.

Received: April 28, 2021; Revised: July 22, 2021; Accepted: July 24, 2021

The objective of the experimental work is to enhance the machining capability of electrical discharge machining by suspending equal proportion of metal powders such as, molybdenum, nickel, and chromium in EDM 30 oil. Three different control factors such as peak current, pulse on time and powder concentration were varied to analyze the response factors namely material removal rate, surface roughness and radial overcut. The cause of powders concentration on material removal rate (MRR), surface roughness (SR), and radial overcut (ROC) have been investigated. An electron dispersive spectroscopy was utilized to investigate the surface revealed the deposition of nickel and chromium in the machined surface. Machined surface was focused to atomic force microscopy and scanning electron microscopy. Analysis of variance (ANOVA) results showed that peak current is the foremost factor in affecting MRR, SR and ROC.

Keywords*: Powder mixed EDM, Rene 41, Radial overcut, Atomic force microscopy, Powder concentration.*

Introduction

Electrical discharge machining process (EDM) is an unconventional process becomes familiar due to their unique merits over other machining process. Conductive materials of any hardness could be cut[1] EDM is a process that uses a regulated applications and there is no vibration, mechanical stress and chatter during machining[2]. Conventional machining process faced difficult to make intricate shapes and cavities, whereas EDM proved as a suitable process to achieve intricate shapes easily. Inconel, Nimonic, Rene, Uidmet and Pyromet are the commercial available alloy. Nickel based super alloy, Rene 80, possess high temperature strength, oxidation resistance, corrosion resistance and chemically stability. Nickel based super alloy's machinability is poor due to various reasons namely, rapid work hardening ability, hard carbides causes abrasion wear, excess spalling and poor diffusivity of nickel alloy[3,4]. Rene 41 and Rene 45 are the commercial available nickel based super alloy.

Powder mixed EDM (PMEDM) is the process of mixing powder in dielectric fluid to improve the capabilities of EDM by increasing the breakdown potential of dielectric fluid[5,6]. Kerosene was used as dielectric and graphite powder was mixed in dielectric to reduce the breakdown potential in order to achieve high MRR[7]. Contrary to this, another investigation did not shown any chemical reaction while using graphite powder with dielectric[8]. Nano alumina powder inclusion in dielectric caused better surface topography with major reduction in micro crocks[9] Quality of the surface was determined by crack density, refinement of grains, surface texture, micro hardness, and formation of recast-layer[10]. PMEDM of inconel 718 using graphite powder in dielectric resulted in smoother surface finish with less surface crack density. Powder concentration (6g/l) resulted in improves surface topology with lesser residual stress[11]. The higher powder concentration has been reduced the MRR due to agglomeration and bonding of balanced particles in the inter-electrode distance[12]. However, surface roughness (SR) declined to some extent up to certain powder concentration, and then started to increase with raise in powder concentration[13]. The existence of semi-conductive graphite nano-powders in the dielectric has been proven to greatly improve the surface finish, increase the MRR, and lower the EWR[14]. At particular machining conditions, aluminium and graphite powder offered a enhanced surface finish in EDM of steel than silicon powder[15]. In addition to powder-mixed EDM of various steels, Kung et al.[16] recently investigated the conventional powder-mixed EDM and its outcomes of MRR and EWR were analyzed[17]. The efficiency of the machining was enhanced due to the accumulation of titanium powder during powder mixed EDM of die steels[18]. Normally, the surface texture was affected by white layer thickness. It was reduced in powder mixed machining of silicon steel and substance properties were also enhanced[19]. The surface hardness, white layer thickness and its defects were analyzed in powder mixed EDM using micro size of titanium powders[20]. In powder mixed EDM of die steels, the powder concentration was the most powerful factor on MRR and SR[21]. The surface integrity and Taguchi optimization were investigated on WEDM of Ti-6Al-4V. The surface morphology was better than before wire cutting process[22]. Low discharge energy was provided the better surface finish during WEDM of Monel alloy[23].

*e-mail: sabaree1987@gmail.com

The novelty of work is to focus on the machining behavior of Rene 41 alloy using powder mixed EDM. In addition to that, surface characterization has been investigated using atomic force microscopy and SEM. Elemental powders of molybdenum, nickel and chromium was analyzed through SEM image.The optimal set of factors has been found using Taguchi approach.

2. Materials and Methods

The experimental work was carried out using die sinking EDM machine ECOWIN (Taiwan) make. Rene rectangular plate of dimension 75mm X 50mm X 8mm was considered as the work piece. The cylindrical electrolyte copper rod of diameter 10mm was used as tool electrode. EDM oil was used as the dielectric fluid. Three elemental powders of molybdenum, nickel and chromium were added in equal proportion by weight. The scanning electron microscopy results of molybdenum, nickel and chromium were shown in Figure 1a-c.

The Figure 2 demonstrates the experimental arrangement of PMEDM. The blind hole of 4mm depth was drilled by using copper electrode. The stirrer attached with motor of 1 HP was used to mix the powders homogeneously with dielectric fluid. Heavy debris removed during machining was collected in debris collector. Three input EDM control parameters namely, peak current, pulse on time, and powder concentration were preferred based on the trial runs. The experimental conditions are enlisted in Table 1. An L9 orthogonal Taguchi array was used to conduct the machining process. Three responses for the investigation are surface roughness, material removal rate and radial overcut. The experimental outcomes were evaluated with respect to the control factors and it's shown in Table 2. The average surface roughness (Ra) of the machined surface was measured using Mitutoya SJ 400. Material removal rate was calculated by using Equation 1 and expressed in mm^3/min. Radial overcut was calculated using E 2.

$$\mathrm{MRR} = \frac{\left(W_{loss} \times 1000\right)}{\left(\tilde{n} \times t\right)} \tag{1}$$

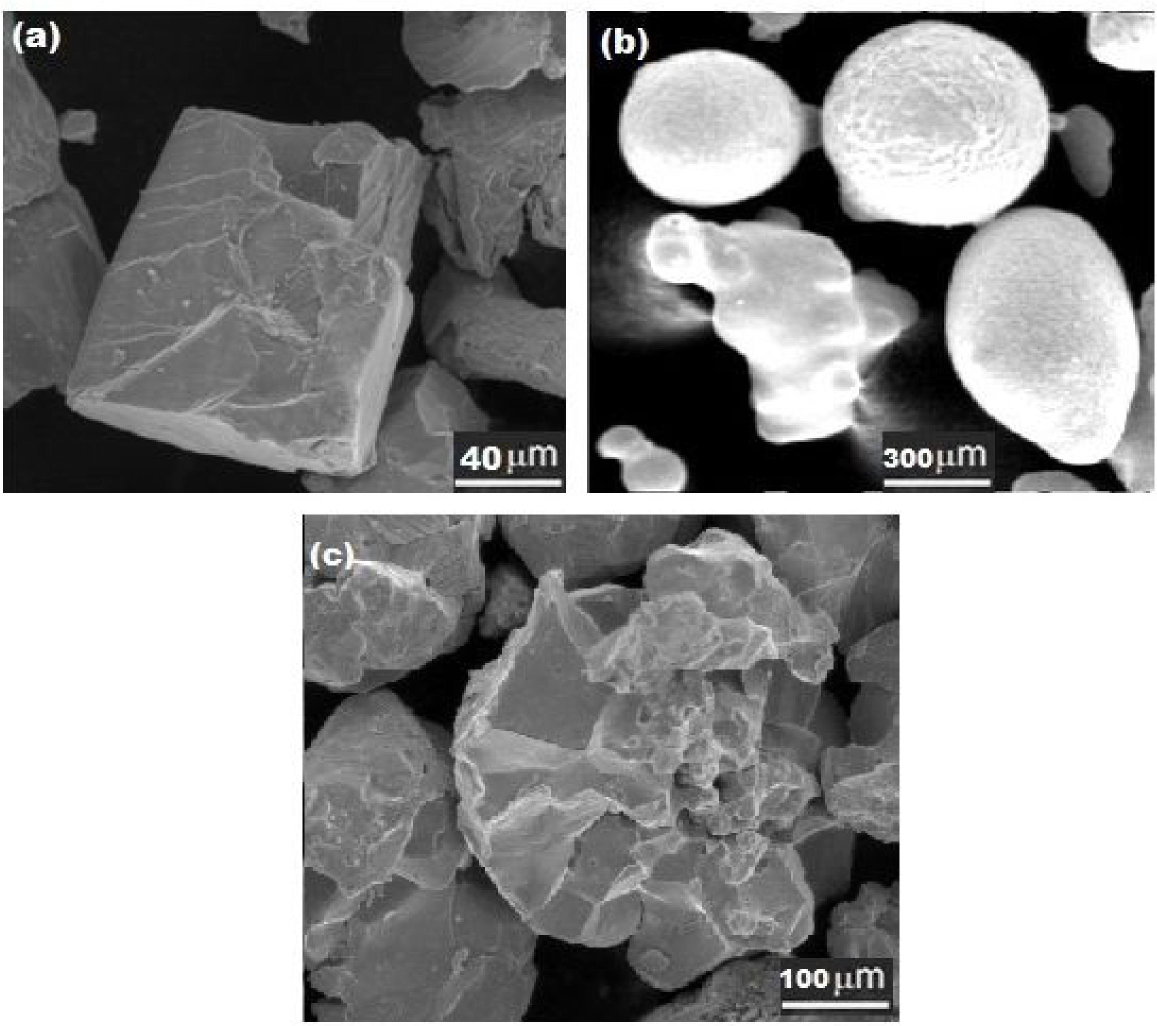

Figure 1. Elemental powders of molybdenum, nickel and chromium.

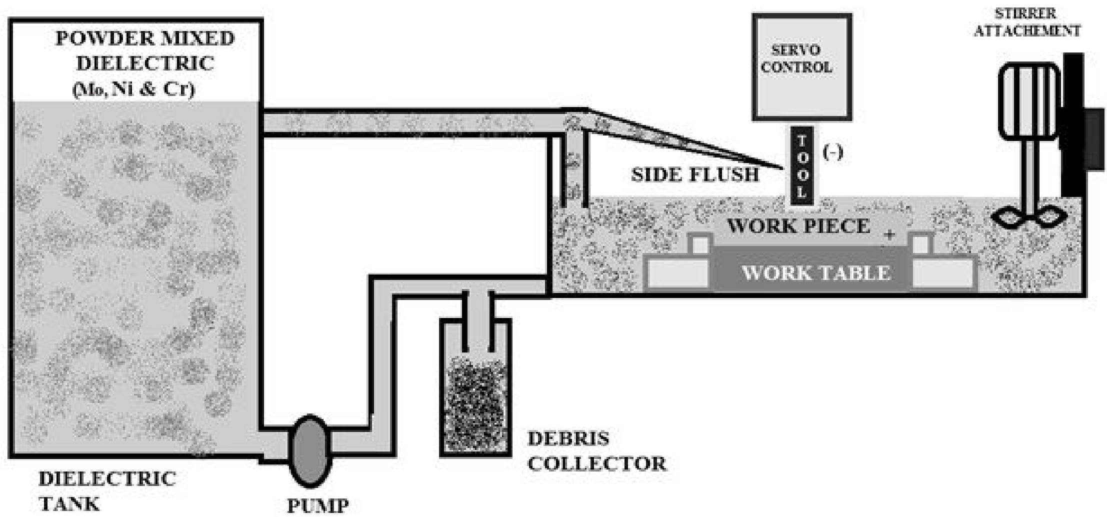

Figure 2. Schematic layout of PMEDM.

Table 1. Experimental conditions for machining on Rene 41.

Machining Condition	Description
Work piece	Rene 45
Tool material	Copper
Powder mixed with dielectric	Molybdenum, nickel and chromium
Polarity	Rene 45 rectangular plate: Positive Copper tool: Negative
Process parameter with their levels	
Peak current	3A, 6A, 9A
Pulse on Time	50µs, 75 µs, 100 µs
Powder Concentration (Al-Ni-Cr)	20 g/lit, 40 g/lit , 60 g/lit
Constant Parameters	
Gap Voltage (V)	50
Duty factor	50%
Spark Gap	0.1mm
Flushing pressure	0.5 kg/cm^2

Table 2. Experimental outcomes.

Run	Peak current	Pulse on time	Powder Concentration	MRR	SR	ROC
1	3	50	20	1.89	3.44	0.027
2	3	75	40	2.19	3.96	0.046
3	3	100	60	4.12	4.42	0.146
4	6	50	40	2.35	5.08	0.048
5	6	75	60	4.76	5.28	0.099
6	6	100	20	5.29	6.44	0.193
7	9	50	60	8.02	6.46	0.124
8	9	75	20	8.56	7.72	0.178
9	9	100	40	7.77	8.46	0.234

Where W_{loss} is weight difference of plate before and after the process which is expressed in mm^3/ min, ρ is the density of the work piece and t is the machining time in minutes.

$$ROC = \frac{D_{bf} - D_{af}}{2} \tag{2}$$

Where D_{bf} is the diameter of the hole produced and D_{af} is the diameter of the tool electrode, respectively.

3. Results and Discussions

3.1 SEM and AFM analysis of machined surfaces

Figure 3a-b shows the SEM results of PMEDM machined surface. From Figure 3a, it is obvious that fused metals melts and immediately cooled down during machining and forms a layer over another layer which results in smooth surface. From Figure 3b, it was clear that machined surface is rough compared to Figure 3a. This is due to the higher peak current as well as higher pulse on time. The particles are uniformly stretched over the surface and the erosion rate is also uniform after the machined surface.

Figure 4 shows the atomic force microscopy result of machined surface at peak current of 3A, pulse on time of 50µs and powder deliberation of 20 gm/lit. It is also evident by 2 dimensional atomic force microscopy results. Atomic force microscopy two dimensional results clearly indicate the presence of smooth surface topology. Figure 5 shows the atomic force microscopy result of machined surface at peak current of 6A, pulse on time of 100µs and powder concentration of 60gm/lit. Figure indicates rough surface formed due to high peak current and high pulse time. Surface morphology is witnessed by peaks and valleys and the two dimensional AFM results also show the surface irregularities. The addition of more powder mixing causes bridging of powder particles. This phenomenon results in formation of carbon on surface of the work piece. As a result, surface roughness gets affected[24].

During the PMEDM of Inconel 718, aluminum powder provided higher MRR than silicon powder when suspended in dielectric due to high amount of energy was transferred through higher thermal and electrical conductivities[25]. MRR increased with the increase of control factor level during Hastelloy PMEDM using aluminum powder suspended dielectric and it's also high discharge energy was produced to the inter-electrode gap[26].

3.2. Taguchi approach

Taguchi approach is one of the best optimization technique used to minimize the number of experimental runs to be carried out within the allowable boundary of

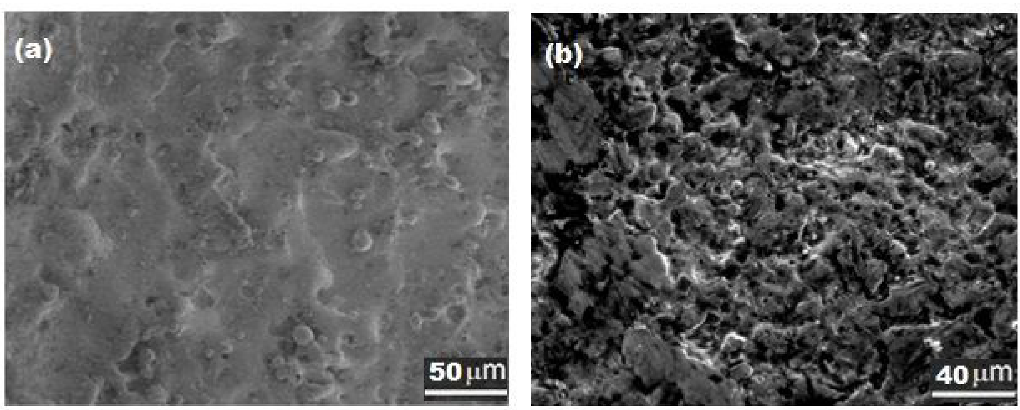

Figure 3. Machined surface at conditions (a) 3A, 50µs and 20gm/lit (b) 9A, 100 µs and 40gm/lit.

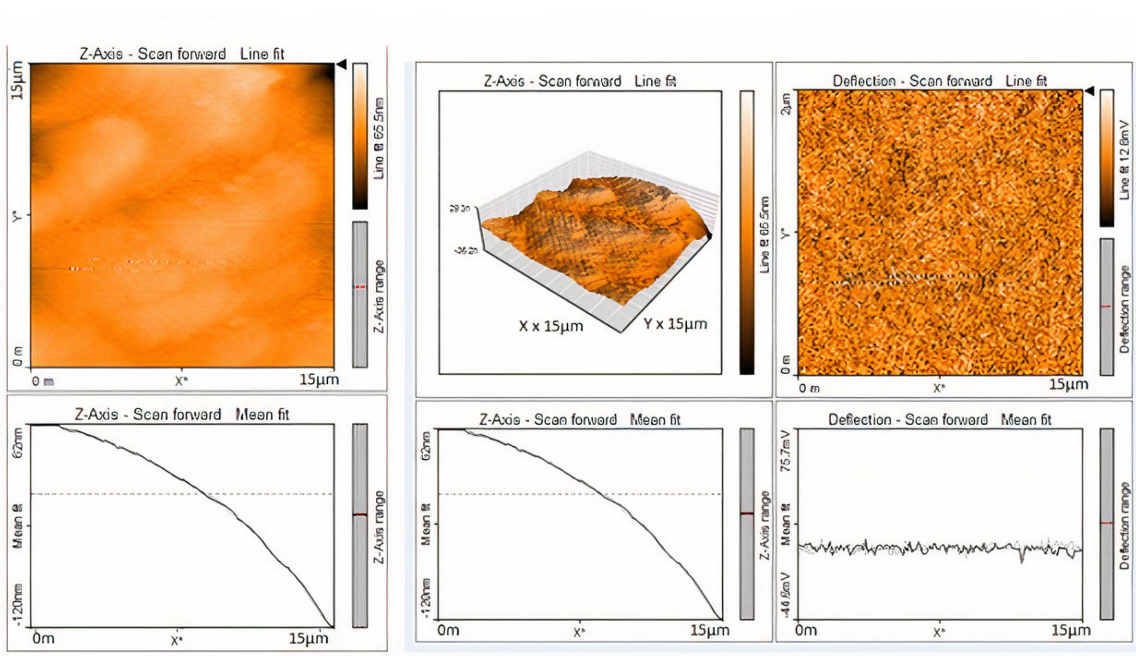

Figure 4. Atomic force microscopy analysis of machined surface at peak current of 3A, pulse on time of 50µs and powder concentration of 20gm/lit.

factors and their levels. Response table for means and SN ratio for MRR, SR and ROC was shown in Table 3. As per lower the better criterion, the means and S/N ratio of SR and ROC was determined. Simultaneously, as per larger the better criterion, the means and S/N ratio of MRR was determined. From the Table 3, it was observed that rank was assigned according to the effect of influential parameter. Influence effect of SN ratio for MRR, SR and ROC was shown in Figure 6a-c. From the figures, the optimal MRR was attained at peak current of 9A, pulse on time of 100µs and powder concentration of 60gm /lit. The optimal SR was attained at peak current of 9A, pulse on time of 100µs and powder concentration of 20gm /lit. The optimal ROC was attained at peak current of 9A, pulse on time of 100µs

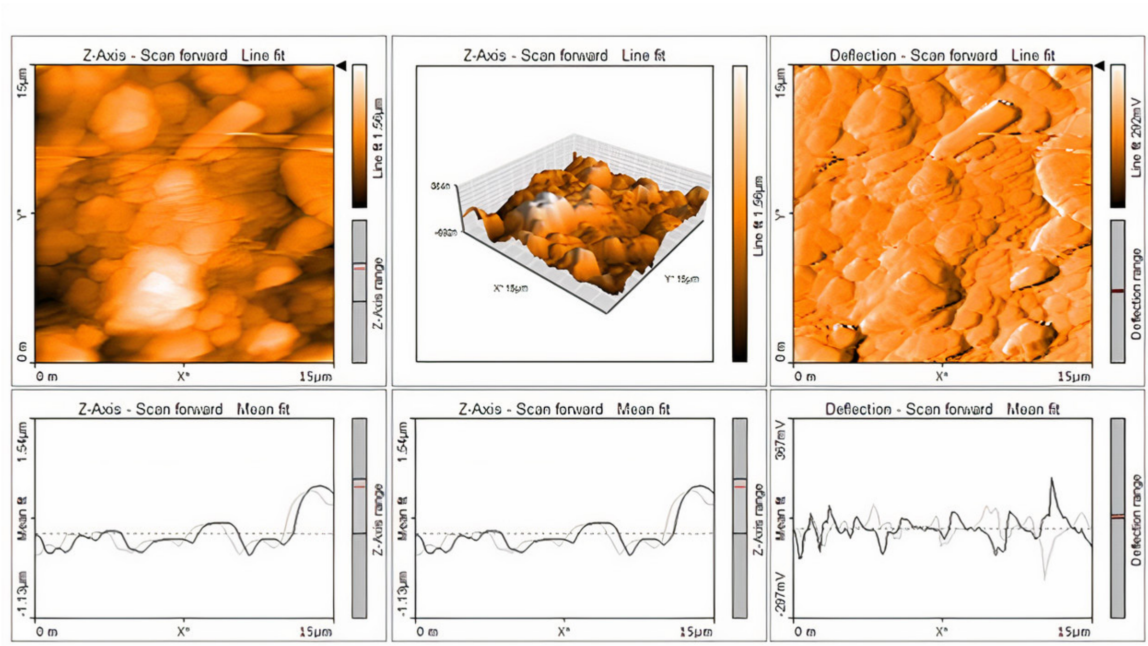

Figure 5. Atomic force microscopy analysis of machined surface at peak current of 9A, pulse on time of 100µs and powder concentration of 40gm/lit.

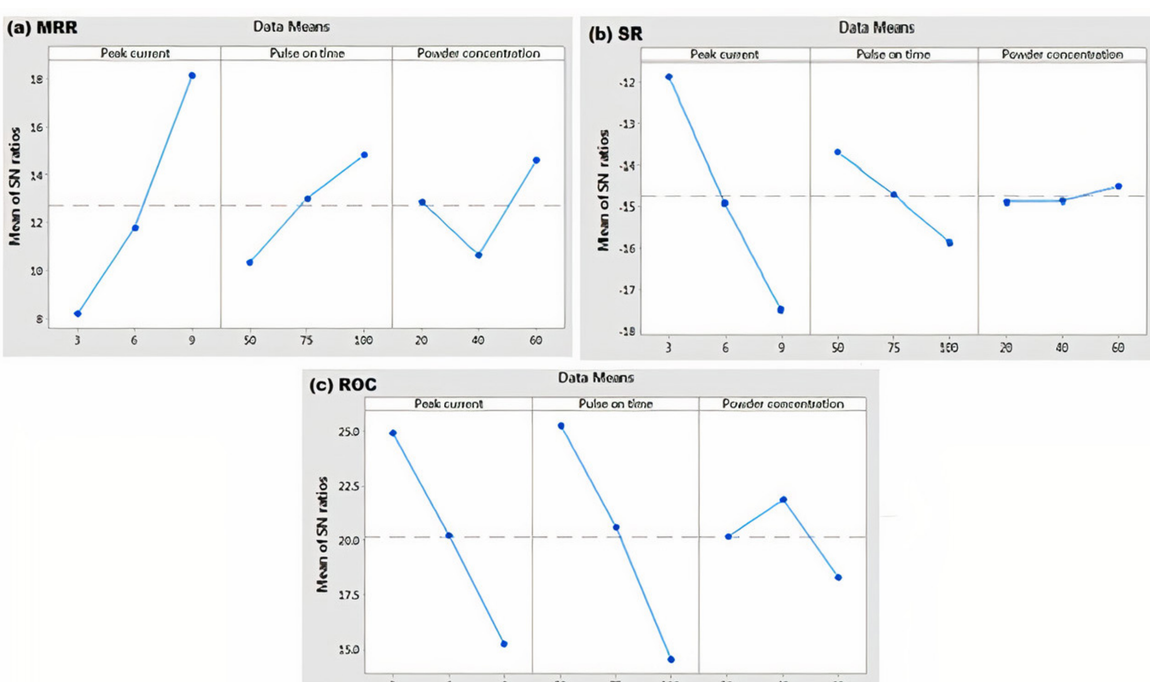

Figure 6. Influence effect of SN ratio for (a) MRR (b) SR and (c) ROC.

and powder concentration of 60gm /lit. Peak current has offered the greatest effect on metal removal and surfaces[18]. The responses and their variation was mainly depends on the quality or objective characteristics[27]

From the Table 4 to 6, it was found that peak current is the predominant factor in affecting MRR, SR, and ROC followed by powder deliberation and pulse on time. All the factors are significant at 95% confidence level. R^2 Higher MRR was achieved at both the higher values of peak current and powder concentration. The increase in powder concentration improves the MRR due to the bridging effect between electrode and workpiece. The bridge chain was formed between the electrode and workpiece which results in dispersion of discharge into several increments and thereby causes more MRR[28]. Further increase in peak current results in release of abundant thermal energy which causes more formation of craters with increased depth. Therefore surface roughness increases[29].Due to higher concentration and localizing of thermal energy in a narrow region leading to higher ROC[30,31]. From Table 4, the contribution of peak current, powder concentration and pulse on time towards MRR were 85.14%, 7.60% and 6.90% respectively. From Table 5, the contribution of peak current, powder concentration and pulse on time towards SR were 84.43%, 13.59% and 1.86% respectively. From Table 6, the contribution of peak current, powder concentration and pulse on time towards ROC were 40.51%, 57.46% and 1.95% respectively.

Table 3. Response table for means and SN ratio for MRR, SR and ROC.

	MRR- SN ratio			MRR- Means		
Level	Current	Powder concentration	Pulse on time	Current	Pulse on time	Powder concentration
1	8.212	10.345	12.883	2.733	4.087	5.247
2	11.814	13.003	10.680	4.133	5.170	4.103
3	18.180	14.858	14.645	8.117	5.727	5.633
Delta	9.968	4.514	3.965	5.383	1.640	1.530
Rank	1	2	3	1	2	3
	SR- SN ratio			SR- Means		
1	-11.86	-13.68	-14.89	3.940	4.993	5.867
2	-14.92	-14.72	-14.87	5.600	5.653	5.833
3	-17.50	-15.88	-14.52	7.547	6.440	5.387
Delta	5.64	2.19	0.37	3.607	1.447	0.480
Rank	1	2	3	1	2	3
	ROC – SN ratio			ROC – Means		
1	24.94	25.29	20.22	0.07300	0.06633	0.13267
2	20.25	20.61	21.91	0.11333	0.10767	0.10933
3	15.25	14.54	18.31	0.17867	0.19100	0.12300
Delta	9.70	10.75	3.60	0.10567	0.12467	0.02333
Rank	2	1	3	2	1	3

Table 4. Variance analysis for MRR.

Source /MRR	DF	SS	MS	F	P	%
Current	2	46.8072	23.4036	239.44	239.44	85.14
Powder concentration	2	4.1731	2.0865	2.0865	0.045	07.60
Pulse on time	2	3.7976	1.8988	19.43	0.049	06.90
Error	2	0.1955	0.0977	--	--	00.36
Total	8	54.9734	--	--	--	100
S= 0.312641	R-sq= 99.64%		R-sq(Adj)= 99.64%		R-sq(Pred)= 92.80%	

Table 5. Variance analysis for SR.

Source /MRR	DF	SS	MS	F	P	%
Current	2	19.5532	9.77658	753.33	0.001	84.43
Powder concentration	2	3.1473	1.57364	121.26	0.008	13.59
Pulse on time	2	0.4310	0.21551	16.61	0.057	01.86
Error	2	0.0260	0.01298	--	--	00.12
Total	8	23.1574	--	--	--	100
S= 0.113920	R-sq= 99.89%		R-sq(Adj)= 99.55%		R-sq(Pred)= 97.73%	

Table 6. Variance analysis for ROC.

Source /MRR	DF	SS	MS	F	P	%
Current	2	0.017061	0.008530	656.18	0.002	40.51
Powder concentration	2	0.024195	0.012097	930.56	0.001	57.46
Pulse on time	2	0.000825	0.000412	31.72	0.031	01.95
Error	2	0.000026	0.000013	--	--	00.08
Total	8	0.042106	--	--	--	100
S= 0.0036056	R-sq= 99.94%		R-sq(Adj)= 99.75%		R-sq(Pred)= 98.75%	

4. Conclusions

- Smooth surface finish of 3.44µm was attained at peak current of 3A, pulse on time of 50 µs and powder concentration of 20gm/lit. From SEM analysis, there was no formation of craters in machined surface.
- Surface irregularity was observed at peak current of 9A, pulse on time of 100µs and powder concentration of 40gm/lit.
- MRR was found to increase with an increase powder concentration from 20gm/lit.
- From Taguchi approach, the optimal MRR was attained at peak current of 9A, pulse on time of 100µs and powder concentration of 60gm /lit.
- The optimal SR was attained at peak current of 9A, pulse on time of 100µs and powder concentration of 20gm /lit.
- The optimal ROC was attained at peak current of 9A, pulse on time of 100µs and powder concentration of 60gm /lit.
- From variance analysis, the involvement of peak current, powder concentration and pulse on time towards MRR were 85.14%, 7.60% and 6.90% respectively and SR were 84.43%, 13.59% and 1.86% respectively.
- The extent of influence of input factors such as current, powder attention and pulse active time towards ROC were 40.51%, 57.46% and 1.95% respectively.

References

1. Abbas NM, Solomon DG, Bahari Md F. A review on current researchtrends in electrical discharge machining (EDM). Int J Mach Tools Manuf. 2007;47:1214-28.
2. Warrier Ashish M, George PM, Raghunath BK, Manocha LM. EDM machining of carbon–carbon composite – a Taguchi approach. J Mater Process Technol. 2004;145:66-71.
3. Richards N, Aspinwall D. Use of ceramic tools for machining nickel-based alloys. Int J Mach Tools Manuf. 1989;29(4):575-88.
4. Ezugwu EO, Wang ZM, Machado AR. The machinability of nickel-based alloys: a review. J Mater Process Technol. 1999;86:1-16.
5. Zhao WS, Meng QG, Wang ZL. The application of research on powder mixed EDM in rough machining. J Mater Process Technol. 2002;129:30-3.
6. Tzeng YF, Lee CY. Effects of powder characteristics on electrodischarge machining efficiency. Int J Adv Manuf Technol. 2001;17:586-92.
7. Jeswani ML. Effect of the addition of graphite powder to kerosene used as the dielectric fluid in electrical discharge machining. Wear. 1981;70(2):133-9. http://dx.doi.org/10.1016/0043-1648(81)90148-4.
8. Sidhu SS, Batish A, Kumar S. Study of surface properties in Particulate-Reinforced Metal Matrix Composites (MMCs) using Powder-Mixed Electrical Discharge Machining (EDM). Mater Manuf Process. 2014;29(1):46-52. http://dx.doi.org/10.1080/10426914.2013.852211.
9. Kumar A, Mandal A, Dixit AR, Das AK. Performance evaluation of Al2O3 nano powder mixed dielectric for electric discharge machining of inconel 825. Mater Manuf Process. 2018;33(9):986-95. http://dx.doi.org/10.1080/10426914.2017.1376081.
10. Kumari S, Datta S, Masanta M, Nandi G, Pal PK. Electro-discharge machining of Inconel 825 super alloy: effects of tool material and dielectric flushing. Silicon. 2018;10(5):2079-99. http://dx.doi.org/10.1007/s12633-017-9728-5.
11. Gangadharudu Talla, Gangopadhyay S, Biswas CK. Influence of graphite powder mixed EDM on the surface integrity characteristics of Inconel 625. Particul Sci Technol. 2017;35(2):219-26. http://dx.doi.org/10.1080/02726351.2016.1150371.
12. Talla G, Sahoo DK, Gangopadhyay S, Biswas CK. Modeling and multi-objective optimization of powder mixed electric discharge machining process of aluminum/alumina/metal matrix composite. Engineering Science and Technology. 2015;18(3):369-73. http://dx.doi.org/10.1016/j.jestch.2015.01.007.
13. Kumar A, Maheshwari S, Sharma C, Beri N. Analysis of machining characteristics in additive mixed electric discharge machining of nickel-based super alloy Inconel718. Mater Manuf Process. 2011;26(8):1011-8. http://dx.doi.org/10.1080/10426914.2010.527415.
14. Jahan MP, Rahman M, Wong YS. Study on the nano-powder-mixed sinking and milling micro-EDM of WC-Co. Int J Adv Manuf Technol. 2011;53:167-80.
15. Jeswani ML. Effects of the addition of graphite powder to kerosene used as the dielectric fluid in electrical discharge machining. Wear. 1981;70:133-9.
16. Kung KY, Horng JT, Chiang KT. Material removal rate and electrode wear ratio study on the powder mixed electrical discharge machining of cobalt-bonded tungsten carbide. Int J Adv Manuf Technol. 2009;40:95-104.
17. Tan PC, Yeo SH, Tan YV. Effects of nano-sized powder additives in micro-electrical discharge machining. Int J Precis Eng Manuf. 2008;9(3):22-6.
18. Marichamy S, Saravanan M, Ravichandran M, Veerappan G. Parametric o ptimization of EDM process on α–β Brass, using taguchi approach. Russ J Non-Ferrous Met. 2016;57(6):586-98.

19. Muthuramalingam T, Phan NH. Experimental investigation of white layer formation on machining silicon steel in PMEDM process. Silicon. 2021;13:2257-63.
20. HuuPhan N, Muthuramalingam T, Vu NN, Tuan NQ. Influence of micro size titanium powder-mixed dielectric medium on surface quality measures in EDM process. Int J Adv Manuf Technol. 2020;109:797-807.
21. Huu P-N. Multi-objective optimization in titanium powder mixed electrical discharge machining process parameters for die steels. Alex Eng J. 2020;59(6):4063-79.
22. Sharma N, Khanna R, Sharma YK, Gupta RD. Multi-quality characteristics optimisation on WEDM for Ti-6Al-4V using Taguchi-grey relational theory. Int J Mach Mach Mater. 2019;21:1-10.
23. Kumar V, Jangra KK. An experimental analysis and optimization of machining rate and surface characteristics in WEDM of Monel-400 using RSM and desirability approach. J Ind Eng Int. 2015;11:297-307.
24. Wu KL, Yan BH, Huang FY, Chen SC. Improvement of surface finish on SKD steel using electro-discharge machining with aluminum and surfactant added dielectric. Int J Mach Tools Manuf. 2005;45:1195-201.
25. Klocke F, Lung D, Antonoglou G, Thomaidis D. The effects of powder suspended dielectrics on the thermal influenced zone by electro discharge machining with small discharge energies. J Mater Process Technol. 2004;149(1–3):191-7.
26. Singh P, Kumar A, Beri N, Kumar V. Influence of electrical parameters in powder mixed electric discharge machining (PMEDM) of hastelloy. J Eng Res Studies. 2010;1(2):93-105.
27. Marichamy S, Ravichandran M, Stalin B, Sridhar Babu B. Optimization of abrasive water jet machining parameters for α-β brass using Taguchi Methodology. FME Transactions. 2019;47:116-22.
28. Zhao WS, Meng QG, Wang ZL. The application of research on powder mixed EDM in rough machining. J Mater Process Technol. 2002;129:30-3.
29. Torres A, Luis CJ, Puertas I. Analysis of the influence of EDM parameters on surface finish, material removal rate, and electrode wear of an INCONEL 600 alloy. Int J Adv Manuf Technol. 2015;80(1-4):123-40. http://dx.doi.org/10.1007/s00170-015-6974-9.
30. Pradhan BB, Masanta M, Sarkar BR, Bhattacharyya B. Investigation on electro-discharge micromachining of titanium super alloy. Int J Adv Manuf Technol. 2009;41(11-12):1094-106.
31. Long BT, Phan NH, Cuong N. Optimization of PMEDM process parameter for maximizing material removal rate by Taguchi's method. Int J Adv Manuf Technol. 2016;87:1929-39.